



## Regular Article

## Heat release at the wetting front during capillary filling of cellulosic micro-substrates



A. Terzis<sup>a,\*</sup>, E. Roumeli<sup>b,c</sup>, K. Weishaupt<sup>d</sup>, S. Brack<sup>a</sup>, H. Aslannejad<sup>e</sup>, J. Groß<sup>f</sup>, S.M. Hassanizadeh<sup>e</sup>, R. Helmig<sup>d</sup>, B. Weigand<sup>a</sup>

<sup>a</sup> Institute of Aerospace Thermodynamics, University of Stuttgart, 70569 Stuttgart, Germany

<sup>b</sup> Department of Engineering and Applied Science, California Institute of Technology, 91125 Pasadena, USA

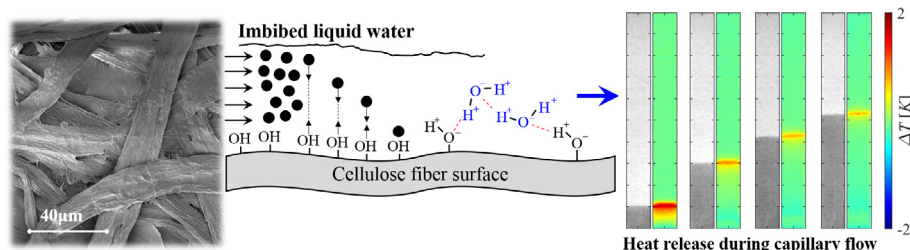
<sup>c</sup> Department of Mechanical and Process Engineering, ETH Zurich, 8092 Zurich, Switzerland

<sup>d</sup> Department of Hydromechanics and Modelling of Hydrosystems, University of Stuttgart, 70569 Stuttgart, Germany

<sup>e</sup> Department of Earth Sciences, University of Utrecht, 3584 CD Utrecht, The Netherlands

<sup>f</sup> Inst. of Thermodynamics and Thermal Process Engineering, University of Stuttgart, 70569 Stuttgart, Germany

## GRAPHICAL ABSTRACT



## ARTICLE INFO

## Article history:

Received 17 May 2017

Revised 6 June 2017

Accepted 7 June 2017

Available online 8 June 2017

## Keywords:

Paper-based microfluidics

Thermodynamics

Capillary dynamics

Interfacial energy

## ABSTRACT

Spontaneous imbibition in cellulosic materials is an expanding field of research due to the direct applicability in paper-based microfluidics. Here, we show experimentally, using simultaneous thermal and optical imaging that the temperature at the wetting front during capillary filling of paper is temporarily increased, even if the imbibed fluid and the cellulosic substrate are initially at isothermal conditions. Several liquids and two types of filter paper, characterised by scanning electron microscopy (SEM) and X-ray diffraction (XRD) analysis, were investigated demonstrating a significant temperature rise at the wetting front that cannot be neglected from the process. The temperature rise is found to be related to the energetics of imbibition compounds, including acid-base contributions, that result in electrostatic attractions as the liquid molecules are adhered on the fiber surfaces upon capillary contact.

© 2017 Elsevier Inc. All rights reserved.

## 1. Introduction

Since their establishment as a medical diagnostic tool [1,2], paper-based microfluidics received a tremendous attention from physicochemical, biomedical and engineering scientists resulting in a multi-discipline research field that has been regularly

reviewed [3–7]. The functionality of such devices is based on the ability of paper as a porous medium to transport liquid spontaneously due to capillary action driven by interfacial energy differences [8], as thermodynamics drives all systems to a lower energy state. The capillary filling of paper is, however, a complex transport process that involves strong adsorptive interactions at the molecular scale. For substrates that are mainly composed of natural cellulosic fibers [9,10], this is associated with the interactions between the imbibed fluid and the available cellulose chains which have

\* Corresponding author.

E-mail address: [alexandros.terzis@me.com](mailto:alexandros.terzis@me.com) (A. Terzis).

their free hydroxyl groups ( $\text{OH}^-$ ) in an equatorial orientation in the glucopyranose rings [11,12], and hence, readily available for bonding (see cellobiose-inset in Fig. 1). The abundance of polar hydroxyls in these regions results in a chemical polarity that can even align cellulosic derivatives when exposed to an electric field [13–15] while measurements of surface energy evidenced that cellulose fibers are biased towards an electron-donor behaviour [16–20]. That is why cellulose, similar to silica surfaces [21], can be used as a strong adsorbent material [22–24]. At the micro-scale, during capillary filling of paper, a precursor liquid film [25] has been shown to move slightly ahead of the wetting bulk phase onto the fiber surfaces forming a kind of liquid slippage [26]. This is believed to have a direct relation to wettability [27] and depends on the mobility of the first adsorbent liquid-layer molecules that occupy the low energy positions of the solid [28,29]. For short range forces, and based on electron transfer theory [30], as the two phases (solid and liquid) are brought together due to capillary action, a spontaneous charge exchange should take place from one surface to another, including acid-base interactions at the interface [31]. This generates an electrostatic attraction (Coulomb forces) between the now oppositely charged surfaces causing the liquid molecules to adhere on the fiber surfaces. Each adhered molecule is replaced by an adjacent one in the liquid film, and the sequential repeat of the process leads to a film movement [29] on the fiber surface.

Therefore, adsorption always takes place at the wetting front due to interactions between charged and/or uncharged molecules that create a film of the adsorbate (imbibed liquid) on the surface of the adsorbent (cellulosic material), as shown in Fig. 1. Since adsorption is an exothermic reaction, energy should be released, and for liquid water-cellobiose interactions this has been proven by molecular dynamic simulations [32]. The enlargement in Fig. 1 shows an example where water molecules are attached on the fiber surfaces by forming hydrogen bonds with whatever accessible oxygen ( $\text{O}^-$ ) or hydroxyl hydrogen ( $\text{H}^+$ ) of the cellulosic material. Assuming that there are no additional processes that could result in a significant temperature drop, e.g. large evaporation rates at the wetting front, the solid-liquid interactions should result macroscopically in a temporary temperature rise.

Despite the presence of a wealth literature on imbibition kinetics in cellulosic substrates [33–42], that demonstrated also limitations of Lucas-Washburn equation [26,43], the thermal field during an isothermal imbibition process has been generally ignored. However, using thermal imaging, we show that the wetting of the fibers at the liquid front results in a temporary thermal spike similar to the fluctuations observed during infiltration of dry soils [44,45], where this kind of behaviour was assigned to condensation of liquid vapour above the wetting bulk. The temperature rise here is related to the energetics of imbibition interactions, and in particu-

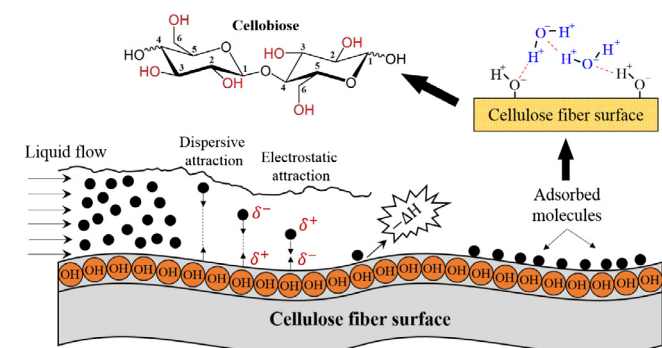


Fig. 1. A schematic representation of the molecular interactions between a cellulosic fiber and imbibed water.

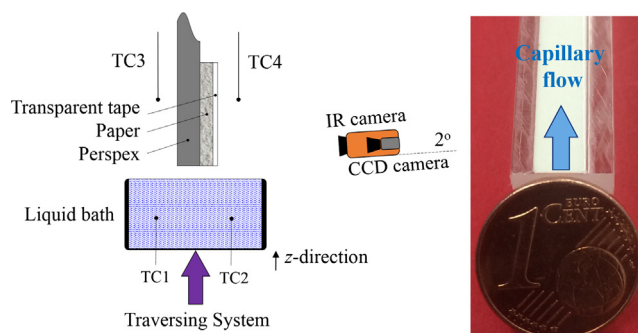


Fig. 2. Experimental apparatus of the imbibition experiments.

lar, to acid-base neutralisation at the interface as the liquid molecules are adsorbed to the solid surfaces during capillary action.

## 2. Experimental section

Fig. 2 shows the experimental apparatus. The overall arrangement consists of an acrylic plate holder where the paper sample is instated, a constant temperature liquid bath placed onto a traversing stage as well as optical and thermal instrumentation. The paper samples were made in  $5 \times 60(\text{mm})^2$  strips, cut in the same direction so that any influence of fiber orientation is the same for all experiments [46]. In order to eliminate liquid evaporation from the wet paper surface, its front side was covered by a clear polypropylene tape of  $50 \mu\text{m}$  thickness that is also transparent to infrared radiation (transmittance 90%). Both edges of the paper-tape packing were carefully trimmed with a cutter in alignment with the acrylic plate. Hence, they were in contact with the atmosphere. The pressure above the wetting front during imbibition was therefore always ambient. The temperatures of the liquid bath, the plate sample and the surroundings were measured with four thermocouples (TC1–TC4), as shown in Fig. 2. The liquid bath was maintained at the same temperature with the paper (room temperature) in order to ensure that no heat is transferred from the bulk liquid to the cellulosic material (and vice versa).

Once isothermal conditions were obtained, the liquid bath was vertically transversed touching the lower edge of the paper initialising imbibition against gravity. Optical and thermal images were then recorded to quantitatively visualise the liquid invasion process. The local temperature distribution was acquired by a FLIR-SC7000C IR camera ( $640 \times 512$ ) and the optical videos with a UI-3360CP CCD camera ( $2048 \times 2048$ ) in the monochrome mode. The IR and CCD cameras were installed in such a distance from the paper sample providing a comparative field of view with a spatial resolution of about  $40 \text{ pixels}/(\text{mm})^2$ . Therefore, each pixel side corresponded to about  $0.156 \text{ mm}$ . Both cameras were set at a constant frame rate of  $4 \text{ Hz}$  while their temporal correlation was accomplished by removing an object of higher temperature in the monitoring frame before each experimental run. The video sequences were therefore synchronised with an accuracy of one frame ( $\pm 0.25 \text{ s}$ ).

## 3. Results and discussion

### 3.1. Optical vs. thermal images

Fig. 3 shows the temporal evolution of optical and thermal images during water uptake in a purely cellulosic paper. At  $t > 0$ , a thermal peak at the same position with the wetting front is observed over the complete video sequence. The temperature spike has the same profile as the water front indicating that heat is

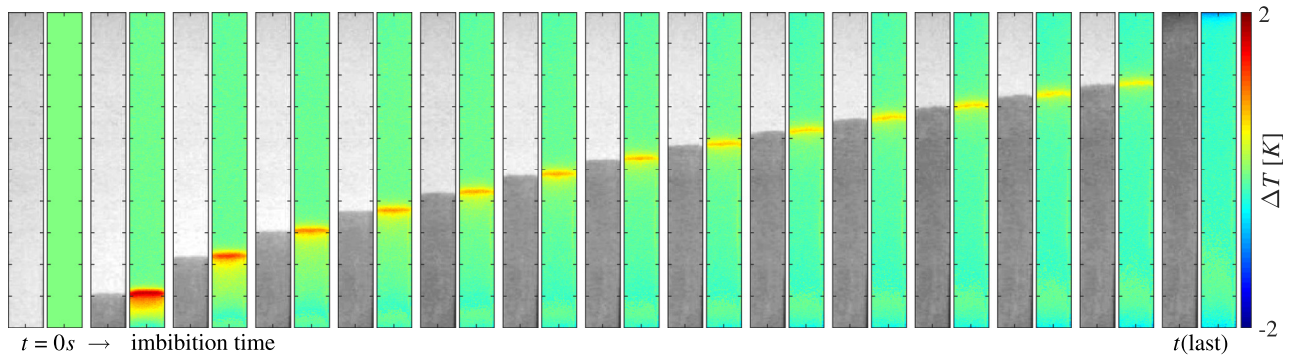


**Fig. 3.** Optical (black-white) and thermal (coloured) images of paper capillary filling with distilled water indicate a heat release at the wetting front. Paper substrate consists of a purely cellulosic material. Consecutive frames every 20 s.

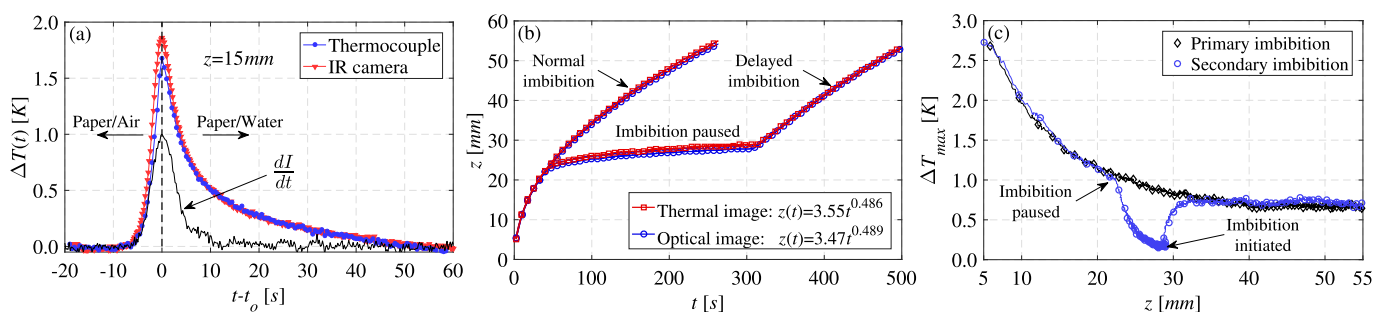
locally released at the interface between the wetting and the non-wetting phases. The magnitude of temperature rise is decreased during imbibition indicating a direct relation to the distributed mass of water. When water rises up in a porous medium spontaneously, the wetting front becomes more diffusive and the corresponding saturation at the front is decreased [47]. The interfacial area where the fiber surfaces are wetted by the liquid is therefore decreased reducing the released energy. As water reaches the top of the sandwiched paper, evaporation starts and a local temperature decrease is observed verifying that evaporation rates during water uptake are minimised by the transparent tape. Fig. 4(a) shows a typical distribution of a thermal peak at  $z = 15$  mm validated with a surface thermocouple. The temperature increases abruptly reaching a maximum point and then converges to the liquid temperature. Both curves exhibit a similar temporal evolution indicating the consistency of the IR measurements while the slightly lower  $\Delta T$  acquired by the temperature sensor is attributed to conduction losses on the thermocouple junction. The first order derivative of the image colour intensity ( $dI/dt$ ), which is dynamically a step response function related to saturation, is also displayed. Clearly, temperature rises when saturation starts to increase reaching a maximum at the same temporal position.

Fig. 4(b) compares the optically and thermally derived wetting fronts illustrating two different experiments. In the first one, named as normal imbibition, water propagates continuously until it reaches the top of the paper. During the second one (delayed imbibition), the water uptake is intentionally paused at 50 s by removing the liquid bath from the bottom of the paper, halting the imbibition process. This causes both the fluid and thermal fronts to stabilise at the same height indicating clearly that the heat is released at the solid-air/solid-liquid interface. The system is left to equilibrate for about 4 min before imbibition is resumed again causing both fronts to propagate together. An excellent

agreement between optically and thermally derived water fronts is observed since both curves follow a Washburn-like scaling law with an average exponent value of  $0.48 (\pm 3\%)$  and an imbibition coefficient of about  $3.50 (\pm 7\%)$  for the primary imbibition curve. Note that the first 5 mm of the water uptake are ignored in order to ensure that any jump of water due to an outside menisci [48] (Wilhelmy force) does not influence the regression fitting. Fig. 4(c) shows the obtained temperature rise for both experimental runs which despite of the low paper thickness exceeds 2.5 K at low imbibition heights. When the imbibition process is interrupted, the heat source is removed and the system is promptly cooled down approaching ambient conditions. However, resumption of the imbibition process causes again a temperature spike which fairly quickly follows the distribution of the normal imbibition curve. These findings demonstrate that any water movement due to capillary action inside the paper microstructure is accompanied by a significant temperature rise at the wetting front.

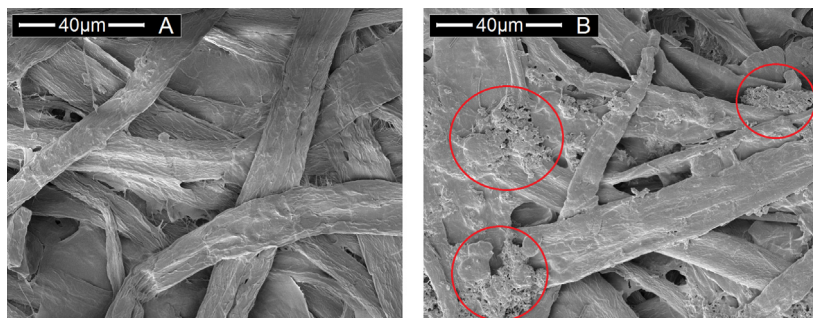
### 3.2. Influence of paper material nature

The influence of substrate material on the temperature rise was examined using a cellulosic paper that is additionally loaded with calcium carbonate ( $\text{CaCO}_3$ ) particles. Its microstructure compared to the purely cellulosic paper is shown in Fig. 5. In both papers, cellulose fibers have an average size of  $12 \mu\text{m}$ . However, the presence of additive particles on Paper-B, marked with red circles, can be identified. The  $\text{CaCO}_3$  fillers influence the cellulosic material nature by modifying the surface charge, and hence, the adsorption capacity of the fibers [49]. In other words, the solid surfaces of Paper-B are energetically more saturated compared to Paper-A. The structural difference between the two papers is further illustrated through the XRD patterns in Fig. 6(a). The characteristic cellulose diffraction peaks are observed for both materials at  $16.5^\circ$ ,  $22.7^\circ$



**Fig. 4.** A quantitative comparison between optical and thermal images (a) validation of IR images with a surface thermocouple and their temporal correlation with the corresponding saturation ( $dI/dt$ ). (b) Washburn-like propagation of the liquid front and the thermal peak (c) maximum temperature rise as a function of imbibition height.





	Paper-A	Paper-B
Material	untreated	CaCO <sub>3</sub> loaded
Density	140g/m <sup>2</sup>	300g/m <sup>2</sup>
Porosity	0.59	0.41
Thickness	232μm	300μm
Fiber size	12μm	12μm

**Fig. 5.** Scanning electron microscopy (SEM) images of the paper samples visualising their structural difference and the existence of calcium carbonate particles (fillers) on Paper-B. Regions of CaCO<sub>3</sub> particles are circle-marked with red. SEM images were obtained on a FEI Nova Nano SEM 450 operating at 5 kV. The table summarises geometrical characteristics of the paper samples. (For interpretation of the references to colour in this figure legend, the reader is referred to the web version of this article.)

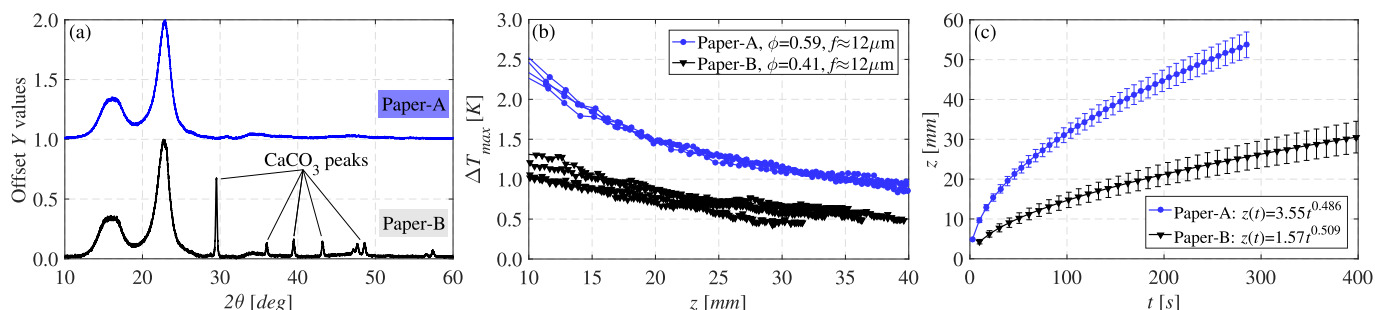


**Fig. 6.** (a) X-ray Diffraction (XRD) patterns of paper samples confirm the cellulosic character of Paper-A as well as the existence of CaCO<sub>3</sub> particles on Paper-B. XRD patterns obtained using a Bruker D8 Advance (CuKα, 40 kV, 40 mA) (b) level of thermal peak as a function of imbibition height. Four individual experimental runs for each paper are displayed. (c) Washburn-like imbibition curves showing the different imbibition coefficient for Paper-A and -B.

and 34.2° [50–52] while Paper-B shows additional peaks at 31°, 36°, 43°, 47.5° and 48.5° verifying the presence of CaCO<sub>3</sub> particles [53–55]. Note also that the available interfacial area between the solid and the liquid is higher for Paper-B due to the similar fiber size and the lower porosity that results in a higher fiber density. Fig. 6(b) shows that  $\Delta T_{max}$  for Paper-B, using water as imbibed liquid, is lower over the complete paper length since  $\Delta T_{max}$  is about 1.4 K and 0.5 K less compared to Paper-A at  $z = 10$  mm and 40 mm, respectively. Both papers are cellulosic, but Paper-B is additionally loaded with CaCO<sub>3</sub> particles which reduce the hydrogen bond opportunities of the solid. Therefore, the solid-liquid interactions during capillary rise generate fewer hydrogen bonds compared to Paper-A which eventually leads to lower temperature rise despite of the larger interfacial area. In other words, Paper-A is more hydrophilic than Paper-B. The higher affinity of Paper-A for water is also reflected in the imbibition rates shown in Fig. 6(c); water uptake is significantly lower for Paper-B. Both curves follow a Washburn-like distribution with similar exponent value of about 0.5. However, the imbibition coefficient is 55% lower for Paper-B, as a direct consequence of the different porosity which modifies the permeability of the porous medium.

### 3.3. Influence of imbibed liquid

The effect of imbibed liquid is investigated on the purely cellulosic substrate (Paper-A). Fig. 7 shows optical and thermal images for various liquids at  $t = 30$  s. As expected, the Washburn-like imbibition rate,  $z^2/t \sim \gamma_l \cos \theta / \eta$ , differs for the different liquids since some fluids propagate faster than others. Pentane, shown in Fig. 7(f), shows the highest imbibition speed due to its very low surface tension ( $\gamma_l = 15.8$  mJ/m<sup>2</sup>) that results in very high wettability affecting dramatically imbibition dynamics [56], while water-ethanol mixture is even slower than pure water. This is due the

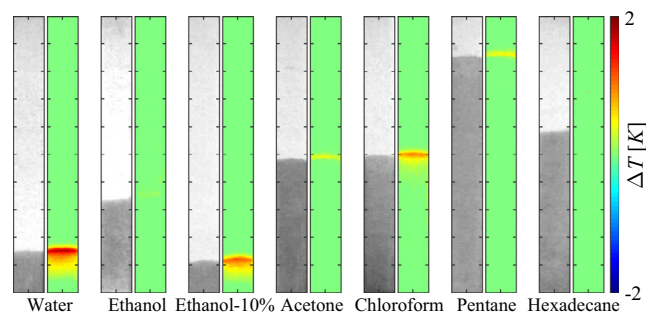


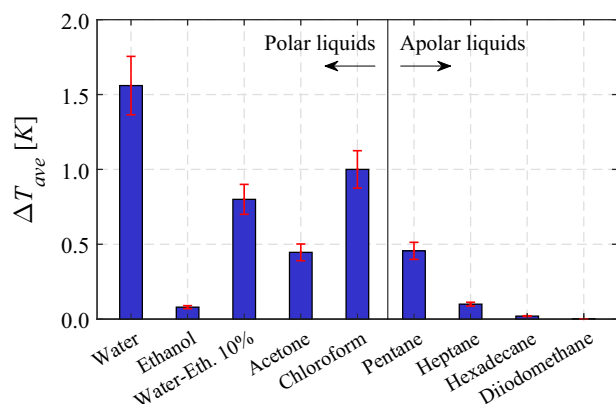
**Fig. 7.** Optical and thermal snapshots of imbibition process for various liquids and Paper-A at  $t = 30$  s.

increase of dynamic viscosity with a small addition of ethanol to pure water [57] accompanied by a reduction of surface tension [58].

Similar to imbibition rates, the temperature rise also differs for various liquids. However, a direct relation to capillary dynamics cannot be made. At a given imbibition time, acetone and chloroform show equal height of rise in paper. However, paper-chloroform interactions provide a significantly higher temperature rise. In addition, pure water shows higher thermal peak and capillary rise compared to water-ethanol mixture. At the same time, liquids such as ethanol and hexadecane do not provide any detectable temperature rise. The temperature rise at the wetting front of various liquids can be explained with the acid-base interactions between compound phases [59,60]. This theory successfully described adsorption processes on activated carbons [61,62] and proteins in aqueous media [63], while the donor-acceptor interactions have been suggested as a strong adsorption mechanism [64,65]. Each liquid has a different potential for acid-base

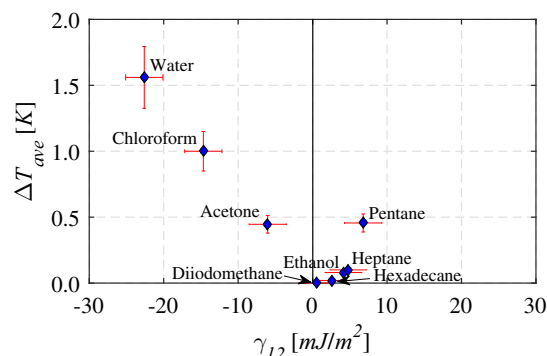
**Table 1**Surface energy components of the used substances. LW and AB correspond to the Lifshitz van der Waals (dispersive) and acid-base contribution to surface energy.  $\gamma^{AB} = 2\sqrt{\gamma^+ \gamma^-}$ .

$\gamma_i$ in mJ/m <sup>2</sup>	$\gamma_i$	$\gamma_i^{LW}$	$\gamma_i^{AB}$	$\gamma_{acid}^+$	$\gamma_{base}^-$
Water	72.8	21.8	51.0	34.2	19.0
Chloroform	27.2	27.2	0.00	1.50	0.00
Ethanol	21.4	18.2	2.40	0.02	68.0
Pentane	15.8	15.8	0.00	0.00	0.00
Heptane	20.4	20.4	0.00	0.00	0.00
Hexadecane	27.5	27.5	0.00	0.00	0.00
Diiodomethane	50.8	50.8	0.00	0.01	0.00
Cellulose (Paper-A)	41.4	40.0	1.40	0.01	50.0

**Fig. 8.** Average temperature rise for the complete wetting of the paper samples for various fluids indicating also the difference in heat release between polar and apolar liquids.

interactions according to its electron acceptor ( $\gamma^+$ ) and donor ( $\gamma^-$ ) contributions to surface energy. These values, summarised in Table 1, were selected based on a number of literature sources for liquids [66–70] and cellulosic materials [16–20].

In order to compare different liquids, the spatially averaged maximum temperature rise over the complete length of paper samples,  $\Delta T_{ave}$ , is considered representing actually an averaged quantity for the complete wetting of the paper. Fig. 8 shows that water, which is the most polar liquid, provides the highest  $\Delta T_{ave}$  compared to all liquids due to the strong hydrogen bonding with the cellulosic material. Chloroform shows a  $\Delta T_{ave}$  of about 1 K that could be also attributed to hydrogen bonding with the —OH groups of cellulose. The increase of temperature for the slightly polar chloroform (acidic liquid) is, however, significantly higher compared to the more polar ethanol (basic liquid). This indicates the important role that acid-base interactions appear to have on the released energy, evidencing also that cellulosic fibers have a predominant basic characteristic. That is why interactions with ethanol molecules are not favoured and cellulose based adsorbent materials have been successfully used for the dehydration of water-ethanol mixtures [23]. For apolar liquids the solid-liquid interactions are driven by dispersive van der Waals forces which are significantly weaker than polar interactions. No detectable temperature rise was therefore observed for diiodomethane while for saturated hydrocarbons only pentane and heptane provided a measurable  $\Delta T_{ave}$  with a tendency of decreasing temperature rise with the size of the molecule. This can be related to (i) the larger number of molecular interactions for small molecules, since hexadecane is bulkier than cellulose resulting an imperfect molecular packing, as well as to (ii) the increased values of the adsorption equilibrium film pressure of the evaporated liquid vapour [71],  $\pi_e$ , that has to be considered in Young's equation for low surface tension liquids that have the tendency to completely wet solid surfaces [72]. For

**Fig. 9.** Relation between temperature rise and solid-liquid interfacial energy.

$n$ -alkanes,  $\pi_e$  was found to increase with decreasing molecular size (increasing evaporation rate) and is negligible for liquids that form a non-zero contact angle [73].

### 3.4. Relation to interfacial energy

We examine the possibility to describe the temperature rise as a function of a thermodynamic property. According to Israelachvili [74], short range forces that contribute to surface energy and adhesion incorporate also “charge exchange (including acid-base interactions) where the spontaneous transfer of charge from one surface to another, dissimilar, surface generates an electrostatic attraction between the now oppositely charged surfaces”. This reasoning suggests that the more energetically similar are the two compounds the less is their electrostatic attraction since a Lewis neutralisation process cannot take place. The interfacial energy,  $\gamma_{12}$ , between two energetically similar surfaces is zero, and hence,  $\gamma_{12}$  is used to compare the temperature rise for various fluids. As an extension of Fowkes approach [75], the interfacial energy between compounds phases accounting also for acid-base interactions can be defined by the van Oss-Chaudhury-Good theory of wettability as [59]:

$$\gamma_{12} = \gamma_1 + \gamma_2 - 2 \left( \sqrt{\gamma_1^{LW} \gamma_2^{LW}} + \sqrt{\gamma_1^+ \gamma_2^-} + \sqrt{\gamma_1^- \gamma_2^+} \right) \quad (1)$$

For a binary system, e.g. solid-liquid,  $\gamma_{12}$  is an important thermodynamic property since it is directly related to the free energy change per unit area between two molecules of solid 1 immersed in liquid 2.

Fig. 9 shows that the averaged temperature rise during the complete wetting of the paper samples ( $\Delta T_{ave}$ ) is minimised as the solid and liquid phases are energetically similar ( $\gamma_{12} \rightarrow 0$ ). The more compatible the materials are the lower the temperature rise at the wetting front. Therefore, for polar liquids which are biased towards an electron donor behaviour similar to cellulose, e.g. ethanol, a detectable temperature rise was not observed. On the other hand, for liquids that are characterised by an electron acceptor

capacity compared to cellulose, e.g. water and chloroform, a significant temperature rise was observed accompanied by negative interfacial energies. A negative interfacial energy (which may be the result of strong acid-base interactions) is possible at high adsorption energies [76,77] and signifies a hydrophilic repulsion [63,60] which is also related to hydration [78]. This means that cellulose molecules have higher affinity for water than themselves indicating also an advantageous condition for strong adherence [73].

#### 4. Conclusions

Despite the considerable amount of literature focused on imbibition kinetics in cellulosic micro-substrates [1,26,33–42], the thermal field during an isothermal imbibition process has been ignored. However, here we showed that a significant heat release takes place at the interface between the wetting and the non-wetting phases, even if the imbibed liquid the cellulosic substrate are initially at the same temperature. The temperature rise is enormous for the given length scale reaching 3 degrees for water and a purely cellulosic substrate of 242  $\mu\text{m}$  thickness. Similar temperature spikes were observed in large scales during infiltration of dry soils [44,45] and their presence was assigned to condensation of liquid vapour above the wetting bulk. Instead, the temperature rise here takes place directly at the interface of the wetting front and it is the result of solid-liquid interactions as the liquid molecules are adhered on the fiber surfaces during capillary action. The magnitude of temperature rise was found to be mainly driven by the energetics of imbibition compounds, and in particular, by acid-base interactions [59,60] which appear to have a predominant influence on the obtained heat release. Therefore, liquids that can be characterised as Lewis acids (e.g. water and chloroform), interact with the basic cellulosic fibers providing a significant temperature rise. On the other hand, the more energetically similar the liquid and the cellulose are (e.g. ethanol), the lower is the temperature rise. These findings actually demonstrate how a macroscopically observed experimental quantity, e.g. thermal field, is related to interactions on the molecular level. Apart from the great fundamental interest, the above findings open up new prospects for more accurate modelling of imbibition processes since, under certain circumstances, thermodynamic equilibrium at the wetting front cannot be assumed. Furthermore, the direct relation of temperature rise to the energetics of the imbibition compounds generates some expectations for the establishment of a new method in determining surface free energy of porous materials in addition to the classical distance-based imbibition experiments [17,18]. Finally, given that the temperature rise can be related to a prospective liquid concentration, the present study shows also the potential of a temperature-based approach for quantitative diagnostics. For example, using a purely cellulosic substrate, analytes which are energetically similar to cellulose, e.g. glucose, will degrade the obtained temperature rise according to their concentration, while DNA, which is biased towards an electron-acceptor behaviour [79] will enhance it.

#### Acknowledgements

A.T. acknowledges the Alexander von Humboldt (AvH) foundation for the funding support. In addition, H.A. and S.M.H. are grateful to the European Research Council (ERC) for the financial support under the ERC Grant Agreement No. 341225. The authors thank also Prof. Jens von Wolfersdorf, Prof. Johannes Kästner, Elmar Sauer and Katharina Heck from University of Stuttgart for their useful discussions as well as to the reviewers who improved the quality and clarity of the paper.

#### References

- [1] A.W. Martinez, D.S.T. Phillips, D.M.J. Butte, P.G.M. Whitesides, Patterned paper as a platform for inexpensive, low volume, portable bioassays, *Angew. Chem. (Int. Ed. Engl.)* 46 (8) (2007) 1318–1320.
- [2] A.W. Martinez, S.T. Phillips, G.M. Whitesides, E. Carrilho, Diagnostics for the developing world: microfluidic paper-based analytical devices, *Anal. Chem.* 82 (1) (2010) 3–10.
- [3] X. Li, D.R. Ballerini, W. Shen, A perspective on paper-based microfluidics: current status and future trends, *Biomicrofluidics* 6 (1) (2012) 011301.
- [4] A.K. Yetisen, M.S. Akram, C.R. Lowe, Paper-based microfluidic point-of-care diagnostic devices, *Lab on a Chip* 13 (12) (2013) 2210–2251.
- [5] E.K. Sackmann, A.L. Fulton, D.J. Beebe, The present and future role of microfluidics in biomedical research, *Nature* 507 (7491) (2014) 181–189.
- [6] D.M. Cate, J.A. Adkins, J. Mettakoonpitak, C.S. Henry, Recent developments in paper-based microfluidic devices, *Anal. Chem.* 87 (1) (2015) 19–41.
- [7] Y. Yang, E. Noviana, M.P. Nguyen, B.J. Geiss, D.S. Dandy, C.S. Henry, Paper-based microfluidic devices: emerging themes and applications, *Anal. Chem.* 89 (1) (2016) 71–91.
- [8] S.M. Hassanizadeh, W.G. Gray, Thermodynamic basis of capillary pressure in porous media, *Water Resour. Res.* 29 (10) (1993) 3389–3405.
- [9] R. Pelton, Bioactive paper provides a low-cost platform for diagnostics, *TrAC Trends Anal. Chem.* 28 (8) (2009) 925–942.
- [10] Y. Xia, J. Si, Z. Li, Fabrication techniques for microfluidic paper-based analytical devices and their applications for biological testing: a review, *Biosens. Bioelectron.* 77 (2016) 774–789.
- [11] C. Yamane, T. Aoyagi, M. Ago, K. Sato, K. Okajima, T. Takahashi, Two different surface properties of regenerated cellulose due to structural anisotropy, *Polym. J.* 38 (8) (2006) 819–826.
- [12] Y. Habibi, L.A. Lucia, O.J. Rojas, Cellulose nanocrystals: chemistry, self-assembly, and applications, *Chem. Rev.* 110 (6) (2010) 3479–3500.
- [13] B. Frka-Petesic, B. Jean, L. Heux, First experimental evidence of a giant permanent electric-dipole moment in cellulose nanocrystals, *EPL (Europhys. Lett.)* 107 (2) (2014) 28006.
- [14] K.J. De France, K.G. Yager, T. Hoare, E.D. Cranston, Cooperative ordering and kinetics of cellulose nanocrystal alignment in a magnetic field, *Langmuir* 32 (30) (2016) 7564–7571.
- [15] S. Rajala, T. Sipponkoski, E. Sarlin, M. Miettinen, M. Vuoriluoto, A. Pammo, J. Juuti, O.J. Rojas, S. Franssila, S. Tuukkanen, Cellulose nanofibril film as a piezoelectric sensor material, *ACS Appl. Mater. Interf.* 8 (24) (2016) 15607–15614.
- [16] F. Dourado, F.M. Gama, E. Chibowski, M. Mota, Characterization of cellulose surface free energy, *J. Adhes. Sci. Technol.* 12 (10) (2012) 1081–1090.
- [17] D.F. Steele, R.C. Moreton, J.N. Staniforth, P.M. Young, M.J. Tobyn, S. Edge, Surface energy of microcrystalline cellulose determined by capillary intrusion and inverse gas chromatography, *AAPS J.* 10 (3) (2008) 494–503.
- [18] I. Pezron, A. Rochex, J.M. Lebeault, D. Clause, Determination of cellulose surface energy by imbibition experiments in relation to bacterial adhesion, *J. Dispers. Sci. Technol.* 25 (6) (2008) 781–787.
- [19] A.F. Miller, A.M. Donald, Surface and interfacial tension of cellulose suspensions, *Langmuir* 18 (26) (2002) 10155–10162.
- [20] P.E. Luner, E. Oh, Characterization of the surface free energy of cellulose ether films, *Coll. Surf. A: Physicochem. Eng. Aspects* 181 (1–3) (2001) 31–48.
- [21] S.K. Parida, S. Dash, S. Patel, B.K. Mishra, Adsorption of organic molecules on silica surface, *Adv. Coll. Interf. Sci.* 121 (1–3) (2006) 77–110.
- [22] B. Acemioglu, M.H. Alma, Equilibrium studies on adsorption of Cu(II) from aqueous solution onto cellulose, *J. Coll. Interf. Sci.* 243 (1) (2001) 81–84.
- [23] T.J. Benson, C.E. George, Cellulose based adsorbent materials for the dehydration of ethanol using thermal swing adsorption, *Adsorption* 11 (1) (2005) 697–701.
- [24] S. Hokkanen, A. Bhatnagar, M. Sillanpää, A review on modification methods to cellulose-based adsorbents to improve adsorption capacity, *Water Res.* 91 (2016) 156–173.
- [25] M.N. Popescu, G. Oshanin, S. Dietrich, A.-M. Cazabat, Precursor films in wetting phenomena, *J. Phys.: Condens. Matter* 24 (24) (2012) 243102.
- [26] R.J. Roberts, T.J. Senden, K.M. A. M.B. Lyne, Spreading of aqueous liquids in unsized papers is by film flow, *J. Pulp Pap. Sci.* 29 (4) (2003) 123–130.
- [27] R.S. Voronov, D.V. Papavassiliou, L.L. Lee, Review of fluid slip over superhydrophobic surfaces and its dependence on the contact angle, *Indust. Eng. Chem. Res.* 47 (8) (2008) 2455–2477.
- [28] A. Martini, A. Roxin, R.Q. Snurr, Q. Wang, S. Lichter, Molecular mechanisms of liquid slip, *J. Fluid Mech.* 600 (2008) 257–269.
- [29] Y. Xue, Y. Wu, X. Pei, H. Duan, Q. Xue, F. Zhou, How solid-liquid adhesive property regulates liquid slippage on solid surfaces?, *Langmuir* 31 (1) (2015) 226–232.
- [30] R.A. Marcus, Electron transfer reactions in chemistry. Theory and experiment, *Rev. Mod. Phys.* 65 (3) (1993) 599–610.
- [31] G.M. Whitesides, H.A. Biebuyck, J.P. Folkers, Acid-base interactions in wetting, *J. Adhes. Sci. Technol.* 5 (1) (1991) 57–69.
- [32] A. Chami Khazraji, S. Robert, A. Chami Khazraji, S. Robert, Self-assembly and intermolecular forces when cellulose and water interact using molecular modeling, *J. Nanomater.* 2013 (4633) (2013) 1–12.
- [33] E. Elizalde, R. Urteaga, C.L.A. Berli, Precise capillary flow for paper-based viscometry, *Microfluid. Nanofluid.* 20 (10) (2016) 135.
- [34] N. Walji, B. MacDonald, Influence of geometry and surrounding conditions on fluid flow in paper-based devices, *Micromachines* 7 (5) (2016) 73.



- [35] Z. Liu, J. Hu, Y. Zhao, Z. Qu, F. Xu, Experimental and numerical studies on liquid wicking into filter papers for paper-based diagnostics, *Appl. Therm. Eng.* 88 (2015) 280–287.
- [36] S. Hong, W. Kim, Dynamics of water imbibition through paper channels with wax boundaries, *Microfluid. Nanofluid.* 19 (4) (2015) 845–853.
- [37] E. Elizalde, R. Urteaga, C.L.A. Berli, Rational design of capillary-driven flows for paper-based microfluidics, *Lab on a Chip* 15 (10) (2015) 2173–2180.
- [38] A. Böhm, F. Carstens, C. Trieb, S. Schabel, M. Biesalski, Engineering microfluidic papers: effect of fiber source and paper sheet properties on capillary-driven fluid flow, *Microfluid. Nanofluid.* 16 (5) (2014) 789–799.
- [39] J. Songok, M. Tuominen, H. Teisala, J. Haapanen, J. Mäkelä, J. Kuusipalo, M. Toivakka, Paper-based microfluidics: fabrication technique and dynamics of capillary-driven surface flow, *ACS Appl. Mater. Interf.* 6 (22) (2014) 20060–20066.
- [40] J. Songok, M. Toivakka, Enhancing capillary-driven flow for paper-based microfluidic channels, *ACS Appl. Mater. Interf.* 8 (44) (2016) 30523–30530.
- [41] A.T. Jafry, H. Lim, S.I. Kang, J.W. Suk, J. Lee, A comparative study of paper-based microfluidic devices with respect to channel geometry, *Coll. Surf. A: Physicochem. Eng. Aspects* 492 (2016) 190–198.
- [42] C. Castro, C. Rosillo, H. Tsutsui, Characterizing effects of humidity and channel size on imbibition in paper-based microfluidic channels, *Microfluid. Nanofluid.* 21 (2) (2017) 21.
- [43] M. Alava, M. Dubé, M. Rost, Imbibition in disordered media, *Adv. Phys.* 53 (2) (2004) 83–175.
- [44] D.M. Anderson, A. Linville, Temperature fluctuations accompanying water movement through porous media, *Science* 131 (3410) (1960) 1370–1371.
- [45] E.R. Perrier, O.M. Prakash, Heat and vapor movement during infiltration into dry soils, *Soil Sci.* 124 (2) (1977) 73.
- [46] A.M. Miranda, I.L. Menezes-Sobrinho, M.S. Couto, Spontaneous imbibition experiment in newspaper sheets, *Phys. Rev. Lett.* 104 (8) (2010) 086101.
- [47] R. Helmig, *Multiphase Flow and Transport Processes in the Subsurface: A Contribution to the Modeling of Hydrosystems*, Springer-Verlag, Berlin, Heidelberg, 1997.
- [48] S. Gruener, T. Hofmann, D. Wallacher, A.V. Kityk, P. Huber, Capillary rise of water in hydrophilic nanopores, *Phys. Rev. E* 79 (6) (2009) 067301.
- [49] P. Fimbel, B. Siffert, Interaction of calcium carbonate (calcite) with cellulose fibres in aqueous medium, *Coll. Surf.* 20 (1–2) (1986) 1–16.
- [50] X. Ju, M. Bowden, E.E. Brown, X. Zhang, An improved X-ray diffraction method for cellulose crystallinity measurement, *Carbohydr. Polym.* 123 (2015) 476–481.
- [51] S. Park, J.O. Baker, M.E. Himmel, P.A. Parilla, D.K. Johnson, Cellulose crystallinity index: measurement techniques and their impact on interpreting cellulase performance, *Biotechnol. Biofuels* 3 (1) (2010) 10.
- [52] H. Zhao, J. Kwak, Z. Conradzhang, H. Brown, B. Arey, J. Holladay, Studying cellulose fiber structure by SEM, XRD, NMR and acid hydrolysis, *Carbohydr. Polym.* 68 (2) (2007) 235–241.
- [53] H. Jia, X. Bai, L. Zheng, Facile preparation of CaCO<sub>3</sub> nanocrystals with unique morphologies controlled by supramolecular complexes, *CrystEngComm* 13 (24) (2011) 7252–7257.
- [54] M. Ni, B.D. Ratner, Differentiating calcium carbonate polymorphs by surface analysis techniques—an XPS and TOF-SIMS study, *Surf. Interf. Anal.* 40 (10) (2008) 1356–1361.
- [55] C.G. Kontoyannis, N.V. Vagenas, Calcium carbonate phase analysis using XRD and FT-Raman spectroscopy, *Analyst* 125 (2) (2000) 251–255.
- [56] A. Clarke, T.D. Blake, K. Carruthers, A. Woodward, Spreading and imbibition of liquid droplets on porous surfaces, *Langmuir* 18 (8) (2002) 2980–2984.
- [57] I.S. Khatlab, F. Bandarkar, M.A.A. Fakhree, Density, viscosity, and surface tension of water+ethanol mixtures from 293 to 323 K, *Korean J. Chem. Eng.* 29 (6) (2012) 812–817.
- [58] G. Vazquez, E. Alvarez, J.M. Navaza, Surface tension of alcohol water + water from 20 to 50 °C, *J. Chem. Eng. Data* 40 (3) (2002) 611–614.
- [59] C.J. Van Oss, R.J. Good, M.K. Chaudhury, Additive and nonadditive surface tension components and the interpretation of contact angles, *Langmuir* 4 (4) (1988) 884–891.
- [60] C.J. Van Oss, Acid-base interfacial interactions in aqueous media, *Coll. Surf. A: Physicochem. Eng. Aspects* 78 (1993) 1–49.
- [61] D.J. de Ridder, A.R.D. Verliefde, K. Schoutteten, B. van der Linden, S.G.J. Heijman, I. Beurroies, R. Denoyel, G.L. Amy, J.C. van Dijk, Relation between interfacial energy and adsorption of organic micropollutants onto activated carbon, *Carbon* 53 (2013) 153–160.
- [62] D.J. de Ridder, A.R.D. Verliefde, B.G.J. Heijman, S. Gelin, M.F.R. Pereira, R.P. Rocha, J.L. Figueiredo, G.L. Amy, H.C. van Dijk, A thermodynamic approach to assess organic solute adsorption onto activated carbon in water, *Carbon* 50 (10) (2012) 3774–3781.
- [63] C.J. Van Oss, *Interfacial Forces in Aqueous Media*, second ed., CRC Press, Taylor & Francis Group, 2006.
- [64] C. Moreno-Castilla, Adsorption of organic molecules from aqueous solutions on carbon materials, *Carbon* 42 (1) (2004) 83–94.
- [65] R. Zhang, B. Li, J. Yang, A first-principles study on electron donor and acceptor molecules adsorbed on phosphorene, *J. Phys. Chem. C* 119 (5) (2015) 2871–2878.
- [66] C. Della Volpe, S. Siboni, Acid-base surface free energies of solids and the definition of scales in the Good-van Oss-Chaudhury theory, *J. Adhes. Sci. Technol.* 14 (2) (2000) 235–272.
- [67] L.-H. Lee, Correlation between Lewis acid-base surface interaction components and linear solvation energy relationship solvatochromic  $\alpha$  and  $\beta$  parameters, *Langmuir* 12 (6) (1996) 1681–1687.
- [68] Q. Shen, On the choice of the acid/base ratio of water for application to the van Oss-Chaudhury-Good combining rules, *Langmuir* 16 (9) (2000) 4394–4397.
- [69] G. Hwang, C.-H. Lee, I.-S. Ahn, B.J. Mhin, Determination of reliable Lewis acid-base surface tension components of a solid in LW-AB approach, *J. Indust. Eng. Chem.* 17 (1) (2011) 125–129.
- [70] Q. Yan, M.-Y. Wang, Y.-H. Wu, L.-H. Jiang, Q. Shen, Electric-assisted capillary rise adsorption of polar and nonpolar solvents by cellulose and chitosan, *J. Phys. Chem. B* 120 (6) (2016) 1121–1125.
- [71] D.H. Bangham, R.I. Razouk, Adsorption and the wettability of solid surfaces, *Trans. Farad. Soc.* 33 (0) (1937) 1459–1463.
- [72] C.J. Van Oss, R.F. Giese, W. Wu, On the degree to which the contact angle is affected by the adsorption onto a solid surface of vapor molecules originating from the liquid drop, *J. Dispers. Sci. Technol.* 19 (6 & 7) (1998) 1221–1236.
- [73] R.J. Good, Contact angle, wetting, and adhesion: a critical review, *J. Adhes. Sci. Technol.* 6 (12) (1992) 1269–1302.
- [74] J.N. Israelachvili, *Intermolecular and Surface Forces*, third ed., sciencedirect.com, 2011.
- [75] F.M. Fowkes, Attractive forces at interfaces, *Indust. Eng. Chem.* 56 (12) (1964) 40–52.
- [76] A. Mathur, P. Sharma, R.C. Cammarata, From our readers: negative surface energy – clearing up confusion, *Nat. Mater.* 4 (3) (2005) 186.
- [77] R.D. Meade, D. Vanderbilt, Origins of stress on elemental and chemisorbed semiconductor surfaces, *Phys. Rev. Lett.* 63 (13) (1989) 1404–1407.
- [78] J. Israelachvili, H. Wennerström, Role of hydration and water structure in biological and colloidal interactions, *Nature* 379 (6562) (1996) 219–225.
- [79] C.J. Van Oss, R.J. Good, M.K. Chaudhury, Mechanism of DNA (southern) and protein (western) blotting on cellulose nitrate and other membranes, *J. Chromatogr. A* 391 (1987) 53–65.